Journal of Catalysis 265 (2009) 181–190

Contents lists available at ScienceDirect

Journal of Catalysis

journal homepage: www.elsevier.com/locate/jcat

Barium-promoted Ru/carbon catalyst for ammonia synthesis: State of the system when operating

Elżbieta Truszkiewicz [a,*], Wioletta Raróg-Pilecka [a], Krzysztof Schmidt-Szałowski [a], Sławomir Jodzis [a], Ewa Wilczkowska [a], Dariusz Łomot [b], Zbigniew Kaszkur [b], Zbigniew Karpiński [b,c], Zbigniew Kowalczyk [a,1]

[a] *Warsaw University of Technology, Faculty of Chemistry, Noakowskiego 3, 00-664 Warsaw, Poland*
[b] *Institute of Physical Chemistry of the Polish Academy of Sciences, Kasprzaka 44/52, 01-224 Warsaw, Poland*
[c] *Faculty of Mathematics and Natural Sciences, Cardinal Stefan Wyszynski University, Dewajtis 5, 01-815 Warsaw, Poland*

ARTICLE INFO

Article history:
Received 19 February 2009
Revised 27 April 2009
Accepted 29 April 2009
Available online 27 May 2009

Keywords:
Ammonia synthesis
Ruthenium catalysts
Graphitized carbon support
Barium promoter
Activation process
Promoter active state

ABSTRACT

The subjects of the research were barium-promoted ruthenium catalysts for ammonia synthesis supported on graphitized carbon. The purpose of this work was to study in detail the process of an active Ba–Ru/C catalyst formation. Another goal was to characterize the active state of the Ba promoter, that is the state corresponding to ammonia synthesis conditions. In situ XRD and TPR–MS techniques were applied to monitor the changes in the Ba–Ru/C specimens when heating in hydrogen (or $H_2 + N_2$) and H_2 + Ar mixtures, respectively. The post-activation state of the catalyst was characterized chemically via interaction of the reduced samples with water vapour at 50 °C and also via interaction with oxygen at 0 °C. The above mentioned experiments were supplemented with those of ammonia synthesis. It was shown that ruthenium facilitates decomposition of the promoter's precursor ($Ba(NO_3)_2$) deposited onto the surface of Ru/C catalysts when heating the specimens in a hydrogen-containing stream. The $Ba(NO_3)_2$/C reference materials, which do not contain ruthenium, are stable in a flowing H_2 + Ar mixture up to about 400 °C, whereas the $Ba(NO_3)_2$ decomposition starts at 100–120 °C in the $Ba(NO_3)_2$–Ru/C systems (XRD, TPR–MS). The decomposition of $Ba(NO_3)_2$ in hydrogen leads to barium oxide (BaO) and metallic barium. Under steady-state conditions BaO is the only Ba-containing phase detected by the X-ray diffraction technique. Characterization of the post-activation catalysts showed that barium is partially reduced during the aforementioned operations and that these catalysts react with oxygen and water vapour. Based on the comparison of the O_2 consumption and H_2 evolution data one may deduce that the active form of the promoter is a mixture: Ba^0 + BaO. It can be stated that the temperature and content of the promoter (C_{Ba}) have a significant influence on NH_3 formation. The shape of reaction rate vs. barium content function is assumed to be an outcome of the promoter distribution on the active carbon surface and ruthenium surface. The trend of the integral reaction rate clearly reflects that of the Ru coverage by the barium-containing species, which is controlled by the heats of adsorption on ruthenium and carbon, respectively.

1. Introduction

Alkali and alkaline earth elements are known to be very efficient promoters for all ammonia synthesis catalysts [1–4]. Potassium and calcium are integral components of the multi-promoted fused iron catalysts used commonly in ammonia plants [5–8]. Cobalt and iron deposited on carbon – both rather poorly active in NH_3 synthesis – become very active upon the addition of barium [9–11] and potassium [12]. Some metal nitrides and ternary nitrides are effectively promoted by caesium [13–16].

Among catalytic systems for NH_3 synthesis, supported ruthenium catalysts represent a novel class of materials that are particularly attractive for commercial application [1,2,17–27]. As unpromoted ruthenium is almost inactive [28], the effect of various additives on the catalytic properties of Ru surfaces in ammonia synthesis has been intensively studied [29]. It has been established by different research groups that caesium and barium are the most advantageous promoters for Ru deposited on magnesia [29–35], magnesium–aluminium spinel [36–39], boron nitride [40–42] or graphitized carbon [17,18,20–23]. In the end of the last century, the Cs- and Ba-promoted Ru catalyst deposited on high-surface area graphite (HSAG) has been implemented successfully by Kellog (Kellog Brown & Root) into the large-scale NH_3 installations operating under low pressure conditions [43,44].

---

[*] Corresponding author.
E-mail address: etruszkiewicz@ch.pw.edu.pl (E. Truszkiewicz).
[1] Deceased.

0021-9517/$ - see front matter © 2009 Elsevier Inc. All rights reserved.
doi:10.1016/j.jcat.2009.04.024

It is commonly assumed that the alkali promotion proceeds via electron transfer from the alkali (caesium and potassium) to the active metal (ruthenium and iron) surface [45–47]. However, there are still doubts regarding the role of barium in an active catalytic system. Barium salts, especially nitrates, are usually the precursors of barium. These salts are introduced into the Ru/C system by impregnation. When such a catalyst precursor is activated in a stream of pure hydrogen and nitrogen, the ruthenium surface is reduced and the salt is decomposed, which results in obtaining the stationary state form of the catalyst. A wide range of research topics which deal with ruthenium-based catalysts doped with barium has been investigated. Despite this fact, few attempts to establish which barium-containing species are present, or where they are localized in the reduced catalyst, have been made [21,27,48,49]. As a consequence, the mechanism of the effect of barium on ruthenium has not been univocally reported. It seems as though the mechanism is strictly related to the state of the promoter under working conditions.

Hansen et al. have performed thorough studies of ruthenium catalysts on different supports (Si_3N_4, $MgAl_2O_4$, BN and C) and on barium-doped systems [39]. Based on the results of HRTEM and EELS studies they stated that in ruthenium systems barium is present in a phase which contains oxygen, i.e. BaO_x. Moreover, the thickness of the layer which this phase forms on the surface of Ru crystallites depends on the support. In the HRTEM photographs no changes in the size of Ru crystallites nor in the structure of the ruthenium surface have been noted as the result of introducing barium. Hence, the authors suggest [39] that barium is an electron donor. Furthermore, they have stated that the magnitude of the observed effect is the larger, the larger the coverage of ruthenium by BaO_x [39]. According to Logadottir et al. [50], BaO_x is located on the ruthenium surface near the active B_5 sites and electrostatically modifies the potential around these sites, making them even more active in N_2 dissociation. Forni et al. are of a similar opinion regarding the form of barium present in the working system [3,51]. Basing on the results of XPS studies of Ba–Ru/C catalysts, the authors [3,51] claim that the active form of the promoter is barium oxide, which acts as an electron donor. The aforementioned statements are also confirmed by Zeng et al. [52]. However, according to him, the barium might not solely be in the form of BaO, but also barium hydroxide ($Ba(OH)_2$). The molar ratio of these two compounds can vary with temperature and the partial pressure of water in the inlet stream. It is noteworthy that higher activities in ammonia synthesis were noted under the conditions under which barium oxide was the predominant barium-containing phase [52]. Although the main effect of barium oxide on the catalyst's activity is associated with electron donation from BaO to Ru, Zeng et al. do not exclude the possibility that it also modifies the ruthenium surface [52]. This means that the overall effect of barium exhibits a dual nature, that is a simultaneous electron and structural promotion [52]. An analysis of XPS studies of a Ba–Ru/C systems led Guraya et al. to conclude that the Ba^{2+} species are not reduced during the catalyst's activation [48]. Therefore, BaO is said to be the working state active phase of the promoter. Moreover, the electronic structure of the Ru/carbon system was not changed by the barium promoter despite the fact that the catalyst was reduced at a high temperature in hydrogen. This indicates that most probably barium is not an electron promoter in ammonia synthesis catalysts [48]. Two other research groups, namely that of Muhler [32] and of Kowalczyk [53], also support the theory that barium exerts a structural effect on the ruthenium catalyst. In the case of supported ruthenium catalysts, barium prevents the ruthenium from sintering, both during the activation and when the catalyst is used [18,23]. Engaging in this kind of interaction is one of the main roles of a structural promoter of a supported catalyst [54].

There is still doubt regarding the chemical form in which barium is in the working state of the catalyst (BaO [27,39,48,51,52], $Ba(OH)_2$ [27,52] or $BaRuO_4$ [54]). As a consequence, there are several opinions as to the mechanism of promotion by barium. It might promote ruthenium structurally [32,33,53], by donating electrons [3,39,40], or in both these ways [52]. This problem is difficult to be solved, due to the fact that there are few methods that can give reliable information about the stationary state of the catalyst under strongly reducing conditions (H_2:N_2 = 3:1, purity >99.9999%, temperature >350 °C).

The aim of this work was to gain insight into the processes that take place during the activation of Ru/C systems doped with barium nitrate. Furthermore, attempts to characterize the stationary state of such catalysts, that is to establish the types of barium-containing species and to localize them, were made. In order to achieve this, the experiments were carried out after a previous long-term activation of these materials in a stoichiometric mixture of hydrogen and nitrogen. These studies are a continuation of our research on the working state of Ru/C systems doped with caesium [55]. The barium-containing systems were analyzed according to the experimental procedure performed on the Cs–Ru/C systems. The activation process was investigated by means of temperature-programmed reduction studies with a simultaneous mass spectroscopy detection (TPR–MS), as well as with *in situ* X-ray diffraction studies. The XRD measurements were carried out using a camera, which was fed with either hydrogen or a stoichiometric hydrogen–nitrogen mixture. The set-up was equipped with a position-sensitive detector. Information regarding the barium-containing species in which the barium is found under the conditions of ammonia synthesis was acquired by two methods, namely by the interaction of the reduced samples with water vapour and by the interaction of the catalyst with oxygen at 0 °C. As in the case of Cs–Ru/C systems [29,55–57], the only source of hydrogen in the experiments with water vapour was Ba in its reduced form (Ba^0), because neither $Ba(OH)_2$ nor BaO can produce H_2 when contacting with H_2O. Although barium hydride could produce hydrogen in this reaction, it is unstable under the catalyst's activation conditions [58]. The amount of hydrogen evolved to the gas phase may be used as a measure of the promoter reduction degree. Oxygen, in turn, may be consumed by the ruthenium surface (chemisorption) and Ba^0, but is inert to the alkali earth metal hydroxides. BaO also does not react with oxygen at 0 °C [58]. The aforementioned characterization experiments were supplemented with those of the catalyst's activity in high-pressure ammonia synthesis. Of particular interest was the effect of Ba loading on the activity, as the promoter state might be correlated with the catalytic properties of the system.

2. Experimental

2.1. Carbon supports, Ba–Ru/carbon catalysts

Two carbon materials, marked throughout the text as A and B, were used as supports for the catalyst preparation. Carbon A was obtained via high-temperature heating (1900 °C, 2 h, helium atmosphere [28]) commercial activated carbon RO 08 supplied by the Norit B.V. Company. The second material (B) was derived from GF 45 starting carbon (Norit B.V.) by its two-step modification consisting of high-temperature treatment (1900 °C, 2 h, He) and a subsequent gasification in a CO_2 stream at approximately 850 °C. After the gasification, the mass loss was 24.6%. Finally, the materials were washed with distilled water and dried in air at 120 °C. Nitrogen physisorption and mercury porosimetry studies have shown (see Table 1) that carbon B exhibits a significantly more developed texture than carbon A.

For Ru/carbon, the supports were impregnated with a THF solution of ruthenium carbonyl (Ru/A) or with an acetone solution of

Table 1
Textural parameters of the carbon supports; S_{BET} – BET surface area; S_{Hg}, V_{Hg}, V_{mHg}- surface area, total volume of pores and volume of pores in the range of 3–100 nm, as determined by mercury porosimetry.

Carbon material	S_{BET} (m^2/g)	S_{Hg} (m^2/g)	V_{Hg} (cm^3/g)	V_{mHg} (cm^3/g)
A	66	60	0.61	0.21
B	1034	192	0.47	0.295

ruthenium chloride (Ru/B). After being dried in air at 60 °C, the samples were reduced in flowing hydrogen of high purity (99.9999%) – first at 150 °C for 24 h and then at 350 °C for 24 h. Next, the material was maintained in a stream of argon, into which air pulses were introduced, and hence the catalyst was passivated. The content of Ru in the Ru/carbon precursors was maintained constant (9.1 wt%).

Barium nitrate, i.e. the Ba precursor, was introduced to the Ru/carbon systems by impregnation from aqueous solutions, followed by drying the samples in air at 90 °C for 24 h. To easily distinguish among the prepared catalysts, all the samples were labelled with unified symbols that specified in sequence: the Ba loading expressed in mmol Ba/$g_{(C+Ru)}$, the Ru loading in the unpromoted system (wt%) and kind of carbon (A, B), e.g. Ba0.81–Ru9.1/B.

2.2. Studies of the catalysts activation

2.2.1. XRD

The experiments were performed in a set-up that enabled studying the specimens under controlled conditions of temperature and gas composition. The main parts of the set-up are a home-built XRD camera, described previously [59], and a position-sensitive detector (PSD). Details about the experimental set-up can be found in our previous paper [55]. The camera was supplied with high purity gases (99.9999% purity). The samples were heated with a linear temperature increase (3 °C/min) in a hydrogen stream (60 ml/min) or in a hydrogen–nitrogen mixture (H_2:N_2 = 3:1; 80 ml/min) up to approximately 520 °C and maintained in that temperature for 15 h. A sequence of the XRD patterns was recorded at intervals of 5 min with a counting time of 3 min for each pattern. The data collection was controlled by a computer programme.

2.2.2. TPR–MS

The set-up for performing the temperature-programmed reduction (activation) experiments, as well as the experimental procedure was described in detail in our previous paper [55]. In brief, the outlet of a tubular flow reactor supplied with a pure 6% H_2/Ar mixture (40 ml/min) was connected via a T-union to the sampling valve of a Dycor Ametek MA 200 quadrupole mass spectrometer. The temperature of the reactor was increased up to 720 °C at a 10 °C/min ramp, whereupon the reduction of the sample was continued. In order to determine the changes in the relative amounts of various species evolving to the gas phase, the obtained MS spectra were elaborated in terms of standard spectra of the respective compounds.

2.3. Characterization studies of the activated catalysts

2.3.1. Interaction with water vapour

Studies of interaction between the reduced catalysts and water vapour were performed in the aforementioned set-up (TPR–MS), using the procedure described in [55]. After the sample reduction (470 °C, 17 h, 80% H_2/Ar, 60 ml/min), the reactor was flushed with argon (40 ml/min) at 430 °C for 30 min to remove hydrogen and then cooled in flowing argon. Subsequently, the Ar stream was replaced with a H_2O/Ar mixture obtained by passing argon through a bubbler filled with redistilled water. Both H_2O and H_2 were monitored with a mass spectrometer after switching from argon to H_2O/Ar; the latter signal (H_2) was used for determining the total amount of hydrogen desorbed to the gas. All the experiments were performed under fixed conditions; the temperature of the bubbler was 40 °C (7% H_2O in a 40 ml/min Ar stream) and that of the reactor was 50 °C, whereas the mass of the catalyst (0.2–0.63 mm particles) was 0.15 g (C + Ru). To avoid water condensation in the set-up, all the relevant tubing, stopcocks and connections were heated.

2.3.2. Interaction with oxygen

The studies were carried out in a conventional, fully automated temperature-programmed set-up (manufactured by Technical University of Łódź), equipped with a U-tube reactor and a TCD cell [4]. Before measurements, the samples were reduced in a H_2:He (80:20) mixture of high purity (99.999%, 40 ml/min) at 430 °C for 17 h (Ru9.1/B sample) or at 470 °C for 17 h (Ba-doped Ru9.1/B). After being flushed with helium at the reduction temperature (40 ml/min, 30 min), the set-up was cooled in He. Then the oxygen uptake at 0 °C was determined by adding small O_2 pulses (6.25 μmol) to the helium stream. The data obtained for the unpromoted samples were used for calculating the ruthenium dispersion expressed as the fraction exposed (FE) and average particle diameter (*d*). The details of such calculations can be found elsewhere [19]. We assumed that the amount of oxygen consumed by the promoter in Ba–Ru/carbon is the difference between the overall O_2 uptake corresponding to Ba–Ru/carbon, and that determined for the unpromoted material. It has already been shown [24,39] that the Ru dispersion remains unchanged upon promotion when its activation is performed under mild conditions.

2.4. Activity studies

The kinetic measurements of ammonia synthesis were carried out in a tubular flow reactor fed with a very pure (H_2O < 0.5 ppm) stoichiometric mixture of hydrogen and nitrogen. The set-up is described in detail elsewhere [60]. Under steady-state conditions of temperature (400 °C or 370 °C), gas flow rate (70 dm^3 [STP]/h) and pressure (63 bar), the concentration of ammonia in the stream leaving the catalyst bed (0.15 g(C + Ru); 0.2–0.63 mm grain size) was monitored. Consequently, we were able to determine the integral reaction rate (productivity) of NH_3 synthesis. Some experiments with an ammonia-rich inlet stream (8.5% NH_3, differential measurements) have also been performed.

Prior to kinetic tests, the $Ba(NO_3)_2$–Ru/carbon samples were reduced (activated) in a stoichiometric H_2 + N_2 mixture, according to the following temperature programme: heating to 400 °C and maintaining at 400 °C for 24 h, heating to 470 °C and maintaining constant temperature for 48 h (*p* = 1 bar). Hence, the activation conditions corresponded to those applied in the characterization studies, that is in interaction with H_2O or O_2 (see above).

3. Results

3.1. Activation process

In situ XRD studies were performed for two $Ba(NO_3)_2$–Ru9.1/carbon samples, which differed only in the type of carbon support. Figs. 1 and 2 show the results of studies of the catalyst based on low-surface carbon A. The measurements were performed in a stream of hydrogen (Fig. 1), as well as in a stoichiometric mixture of hydrogen and nitrogen (Fig. 2). Fig. 3 depicts the diffraction patterns of the system based on high-surface carbon B during its activation in pure hydrogen.

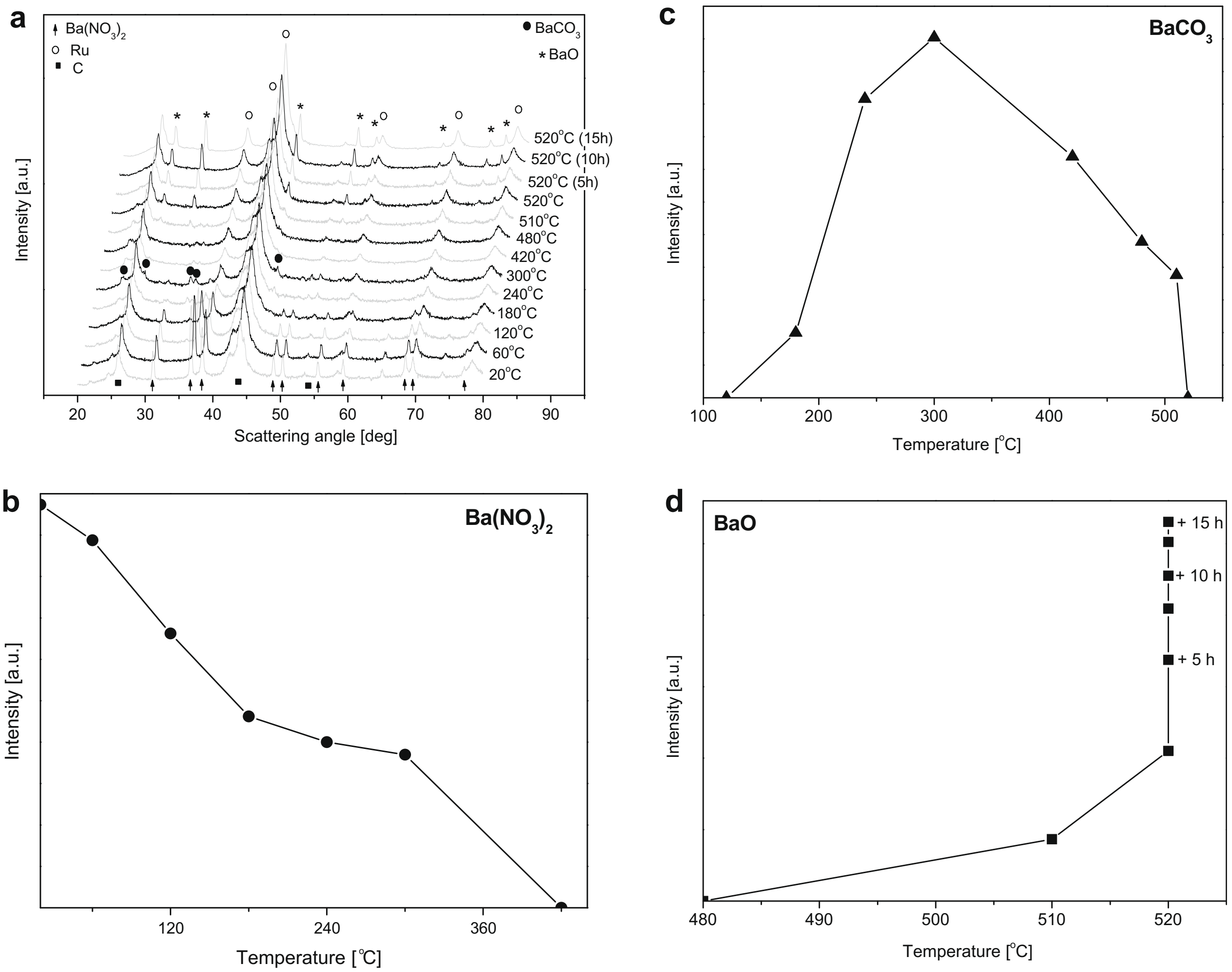

Fig. 1. (a) In situ XRD studies of the Ba0.36–Ru9.1/A specimen; pattern evolution with temperature (H_2: 60 ml/min); (b–d) transformation of barium compounds during the measurement: decomposition of barium nitrate (b), an intermediate $BaCO_3$ phase (c), final product BaO (d).

As shown in Fig. 1, in the diffraction pattern of $Ba(NO_3)_2$–Ru9.1/A, apart from intensive reflections of the precursor of the promoter, i.e. $Ba(NO_3)_2$, signals that come from the carbon support and ruthenium are observed (Fig. 1a). The only changes brought about by the increase of temperature are those of barium-containing species. At approximately 120 °C the decomposition of barium nitrate begins. It terminates at a relatively high temperature, that is approximately 420 °C (see Fig. 1b). According to thermodynamic data, barium nitrate can be reduced to metallic barium ($Ba(NO_3)_2 + 9H_2 = Ba + 2\ NH_3 + 6H_2O$, $\Delta G = -145.4$ kcal) or to barium oxide

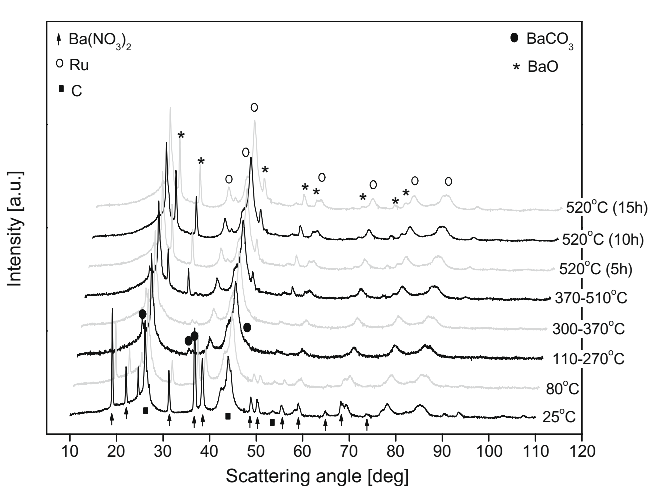

Fig. 2. In situ XRD studies of the Ba0.36–Ru9.1/A specimen; pattern evolution with temperature (H_2: 60 ml/min + N_2: 20 ml/min).

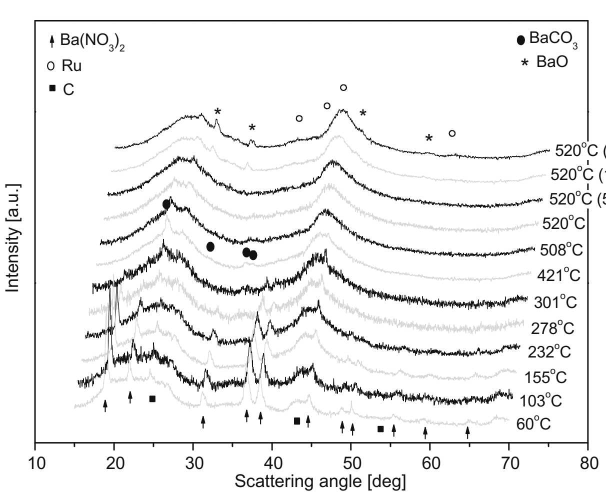

Fig. 3. In situ XRD studies of the Ba0.81–Ru9.1/B specimen; pattern evolution with temperature (H_2: 60 ml/min).

($Ba(NO_3)_2 + 8H_2 = BaO + 2NH_3 + 5H_2O$, $\Delta G = -217$ kcal). However, there are no signals corresponding to these phases, which is probably due to the fact that they are amorphous. Signals from $BaCO_3$ appear and then fade out. The highest intensity of these signals is observed at 300 °C (Fig. 1c). Barium carbonate presumably forms in the reaction between BaO and CO_2 ($BaCO_3 = BaO + CO_2$, $\Delta G = 51.6$ kcal). This indicates that although BaO signals are not visible in the XRD pattern, this phase was formed when barium nitrate decomposed. Carbon dioxide can be produced according to the equation: $2H_2O + C = CO_2 + 2H_2$, or in the reduction of oxygen-containing functional groups which are present on the surface of the support. Then, $BaCO_3$ decomposes into BaO. At approximately 480 °C signals from barium oxide are noted. In the end, the only phase visible in the XRD pattern at 520 °C is BaO, which is stable at this temperature, as shown in Fig. 1d. It is noteworthy that in the three consecutive diffraction patterns, which correspond to 5, 10 and 15 h of maintaining the sample at 520 °C (Fig. 1a), the intensity of the BaO signals increases. This indicates that when the sample is maintained in hydrogen at high temperature (520 °C) for a long time, the structure of the BaO in the sample becomes more ordered.

The changes which $Ba(NO_3)_2$–Ru9.1/A undergoes when heated in a stoichiometric mixture of hydrogen and nitrogen are depicted in Fig. 2. When they are compared to those obtained in a stream of pure hydrogen (Fig. 1), it can be stated that the activation process is the same in both cases. As seen in Fig. 2, the following phases: barium nitrate, barium carbonate and barium oxide, can be clearly distinguished in the appropriate temperature ranges. Signals corresponding to the carbon support and ruthenium are similar in Figs. 1a and 2. Therefore, it can be concluded that the experiments with hydrogen alone give information which is valid for ammonia synthesis conditions.

In contrast to $Ba(NO_3)_2$–Ru9.1/A, $Ba(NO_3)_2$–Ru9.1/B gives only intensive signals of one predominant phase, i.e. the salt of the promoter ($Ba(NO_3)_2$) (Fig. 3). The signals corresponding to carbon and ruthenium are wide and of a low intensity, which indicates that support B is poorly ordered and that the crystallites of the active phase, i.e. Ru, are rather small. The activation of $Ba(NO_3)_2$–Ru9.1/B in hydrogen is analogous to that of the corresponding sample on support A, as the sequence of phase transitions is the same. The discrepancies of the signals in the diffraction patterns are caused only by the difference in the texture of the supports.

Taking everything into account, it can be said that the results of in situ XRD studies of Ru/carbon systems promoted with barium confirm a high thermal stability of the catalysts. When the samples are maintained at 520 °C in a reductive atmosphere, that is either pure hydrogen or a stoichiometric mixture of hydrogen and nitrogen, no significant changes are observed. Regardless of the used carbon support, A or B, barium oxide is the only barium-containing phase whose signals are observed in the XRD patterns at this temperature.

3.1.1. TPR–MS

The TPR–MS studies have been performed on only one system, namely $Ba(NO_3)_2$–Ru9.1/B. This is due to the fact that earlier experiments have shown that in the case of $CsNO_3$–Ru9.1/carbon [55] systems, the type of carbon support does not influence the activation of the catalyst qualitatively. The results obtained when heating the barium-containing sample in a mixture of 6% H_2 in Ar are depicted in Fig. 4. In it, the relations between the time and the concentration of a given component, such as H_2, H_2O, NH_3 and CO, expressed in arbitrary units, are given. The function of temperature in time is also shown.

The hydrogen consumption signal is observed already at 100 °C (Fig. 4). At this temperature in the XRD in situ patterns (Fig. 3), the signals of the promoter's precursor indicate that its decomposition is starting. The consumption of hydrogen is accompanied by the formation of water, ammonia and carbon oxide. These three compounds are the main products of the changes which occur in the sample, similarly as in the case of the Ru/carbon systems doped with caesium [55]. The carbon oxide that evolves can be the product of the reaction: $C + H_2O = CO + H_2$, or is connected with the reduction of oxygen-containing functional groups, e.g. carbonyl or carboxyl groups, which are present on the surface of the support. Apart from H_2O, NH_3 and CO, the outlet stream was also found to contain minute amounts of nitrogen, carbon dioxide and methane (not shown in Fig. 4).

In order to establish the influence of the presence of ruthenium on the activation process of Ba–Ru/carbon systems, an additional TPR–MS measurement has been carried out. The investigated system contained 0.75 mmol barium on carbon B, but no ruthenium. The results of this experiment are presented in Fig. 5. In contrast to the sample which contained ruthenium, the Ba0.75/B sample heated in a mixture of 6% H_2 in Ar did not undergo any changes until the temperature of approximately 400 °C was reached (Fig. 5). At this temperature the consumption of hydrogen begins. Simultaneously, H_2O, NH_3 and CO form. Certain amounts of carbon dioxide and N_2O are also present in the outlet gas. The evolution of these gases ends before the temperature of 500 °C is reached. Then, at temperatures exceeding 500 °C, carbon oxide has been found to evolve again, this time as a result of the decomposition of oxygen-containing functional groups from the surface of the support.

In conclusion, it can be stated that the TPR–MS studies have revealed that ruthenium facilitates the decomposition of barium nitrate. As a consequence, the temperature of barium nitrate decomposition is shifted from 400 to approximately 120 °C. Similar results were obtained by Liang et al. [27]. This is probably the result of the formation of atomic hydrogen [27,52]. The TPR–MS studies of Ba–Ru/carbon systems confirmed their high thermal stability. It is noteworthy that although the temperature exceeded 700 °C, no evolution of methane, i.e. the product of the reaction between hydrogen and the carbon support, has been noted. Barium is therefore an effective inhibitor of methanation. This result is in accordance with the literature data [3,18,51,61].

3.2. Working state of the Ba–Ru/carbon systems

Studies concerning the working state of the catalysts were conducted for a series of samples supported on carbon B. Two catalysts were of the same ruthenium loading (9.1 wt%) but differed in the barium content: 0.36 or 0.81 mmol $Ba/g_{(C+Ru)}$. As the reference materials two Ba/carbon samples without ruthenium, namely Ba0.30/B and Ba0.75/B, were examined. For comparison, the unpromoted Ru9.1/B sample was also used.

3.2.1. Interaction of the reduced catalysts with oxygen

Blank experiments have shown that the carbon support is inert towards oxygen. Therefore, the oxygen consumption of Ru/B was assigned solely to ruthenium. In order to establish how many moles of atomic oxygen (mol O/mol Ba) were consumed by barium in the Ba–Ru/B sample, the assumption that ruthenium exhibits the same oxygen uptake in both promoted and unpromoted samples, has been made. The results of the studies concerning the interaction of these samples with oxygen are shown in Table 2.

As seen in Table 2, the amounts of oxygen consumed by the barium-promoted samples are larger than those corresponding to the unpromoted one. The consumption of the oxygen was 25% higher in the case of the catalyst that contained more barium. Furthermore, when the barium content is increased more than twofold, a smaller amount of oxygen per mole of barium is observed.

Oxygen exhibited reactivity not only towards the catalysts, i.e. Ru/carbon and Ba–Ru/carbon, but also towards the reference

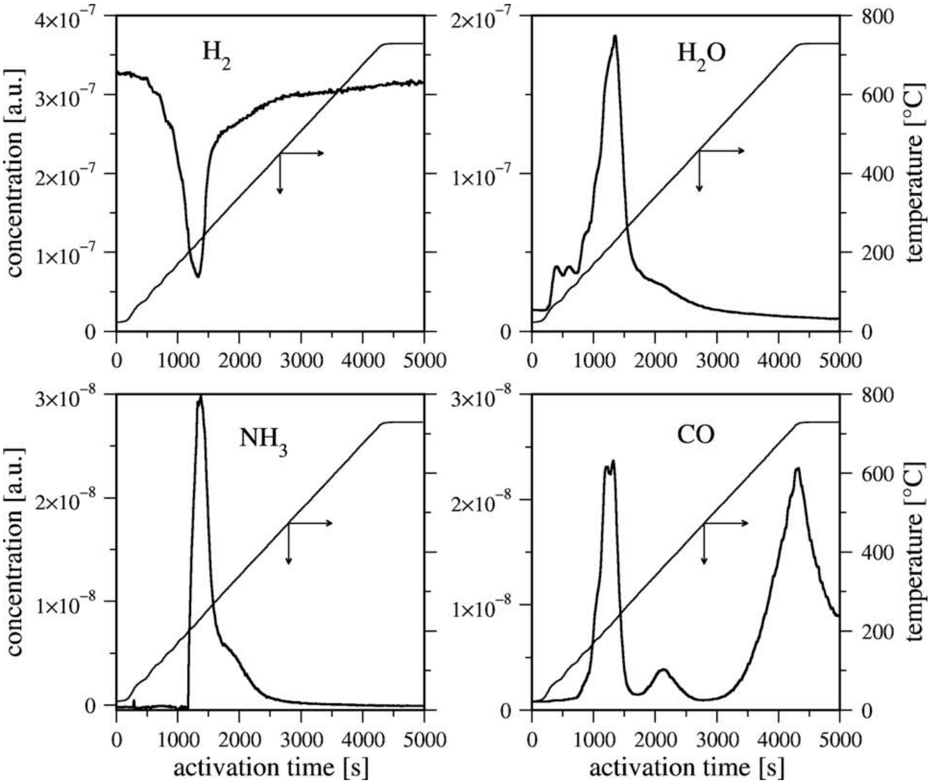

Fig. 4. TPR–MS studies of the $Ba(NO_3)_2$–Ru9.1/B catalyst: concentrations of the main components in the outlet gas stream (6% H_2/Ar, 40 ml/min) and temperature vs. activation time; the starting sample (0.1771 g) contained 0.1328 g carbon, 0.0133 g Ru and 0.0310 g $Ba(NO_3)_2$.

materials, that is Ba/carbon systems, which had previously been heated in hydrogen. In accordance with our expectations, a higher barium content corresponds to a higher oxygen consumption (Table 2). However, the increase in the amount of barium present in the sample causes a decrease in the O/Ba ratio, as in the ruthenium-containing samples (see Table 2). The values are 0.37 and 0.29 for Ba0.30/B and Ba0.75/B, respectively. These values are significantly lower than those obtained for samples containing ruthenium and similar barium loads, namely 0.64 and 0.52 for Ba0.36–Ru9.1/B and Ba0.81–Ru9.1/B, respectively.

The results presented above are difficult to interpret univocally. This is due to the lack of certainty as to the oxidation state of the barium promoter after the reaction of the catalyst with oxygen, and hence, in the working state of the catalyst. However, it can be stated that barium hydroxide is not the only barium-containing phase. If that were the case, the Ba/carbon systems would not react with oxygen because $Ba(OH)_2$ is inert towards this gas. A more detailed discussion of the O_2 sorption results will be presented later on.

3.2.2. Interaction of the catalysts with water vapour

Experiments aimed at establishing the amount of hydrogen evolved as a result of the interaction of reduced samples with water vapour have been conducted. All three types of systems, i.e. Ba/carbon, Ru/carbon and Ba–Ru/carbon, have been tested. MS studies have confirmed the expectation that the only gas that evolves when such samples are treated with water vapour, is hydrogen. The amount of hydrogen formed in each case is presented in Table 3.

As seen in Table 3, the amount of evolved hydrogen in the case of an unpromoted sample, namely Ru9.1/B, was 15 μmol H_2/g_{C+Ru}. This value significantly increased when barium was added into the system. For Ba0.36–Ru9.1/B this figure was 86.5 μmol/g_{C+Ru}. A further increase in the hydrogen evolution was noted when the barium content was increased. The value corresponding to the Ba0.81–Ru9.1/B sample was 154 μmol/g_{C+Ru} (Table 3), which is an order of magnitude higher than that noted for the unpromoted Ru/B system.

Barium present in systems without ruthenium also reacted with water vapour. However, the amount of hydrogen evolved by such a sample is more than 20 times smaller than that which corresponds to the Ba–Ru/carbon systems with a similar barium content (Table 3). It is noteworthy that the increase in the barium content causes a larger hydrogen emission.

The data presented in Table 3 were used, after correction (Ru9.1/B – 15 μmol H_2/g_{C+Ru}) to determine the number of equivalent Ba atoms (Ba^0) responsible for the hydrogen production ($Ba^0 + 2H_2O = Ba(OH)_2 + H_2$). Consequently, the reduction degrees of barium, RD = Ba^0/Ba_{total} were calculated. The results of these calculations show that in Ba–Ru9.1/B systems barium is only partially reduced. However, the RD value is slightly higher than that for the sample with a lower barium content (Table 3). On the reduction of Ba/B systems, barium is also reduced, although the RD value is 20 times smaller than the reduction degrees of the appropriate ruthenium-containing systems. Samples of Ba0.30/B and Ba0.75/B exhibit reduction degrees slightly higher than one percent. It can therefore be stated that ruthenium clearly promotes the reduction of barium nitrate.

3.3. Activity of the catalysts in ammonia synthesis

Kinetic studies have been carried out for a series of catalysts with the barium content ranging from 0.16 to 0.81 mmol Ba/g_{C+Ru}. They were based on the same unpromoted system, namely Ru9.1/B. The activity measurements were carried out under the following conditions: 63 bar at 370 °C and 400 °C. The activities were expressed in terms of the productivity (r_{int}). Furthermore, the reaction

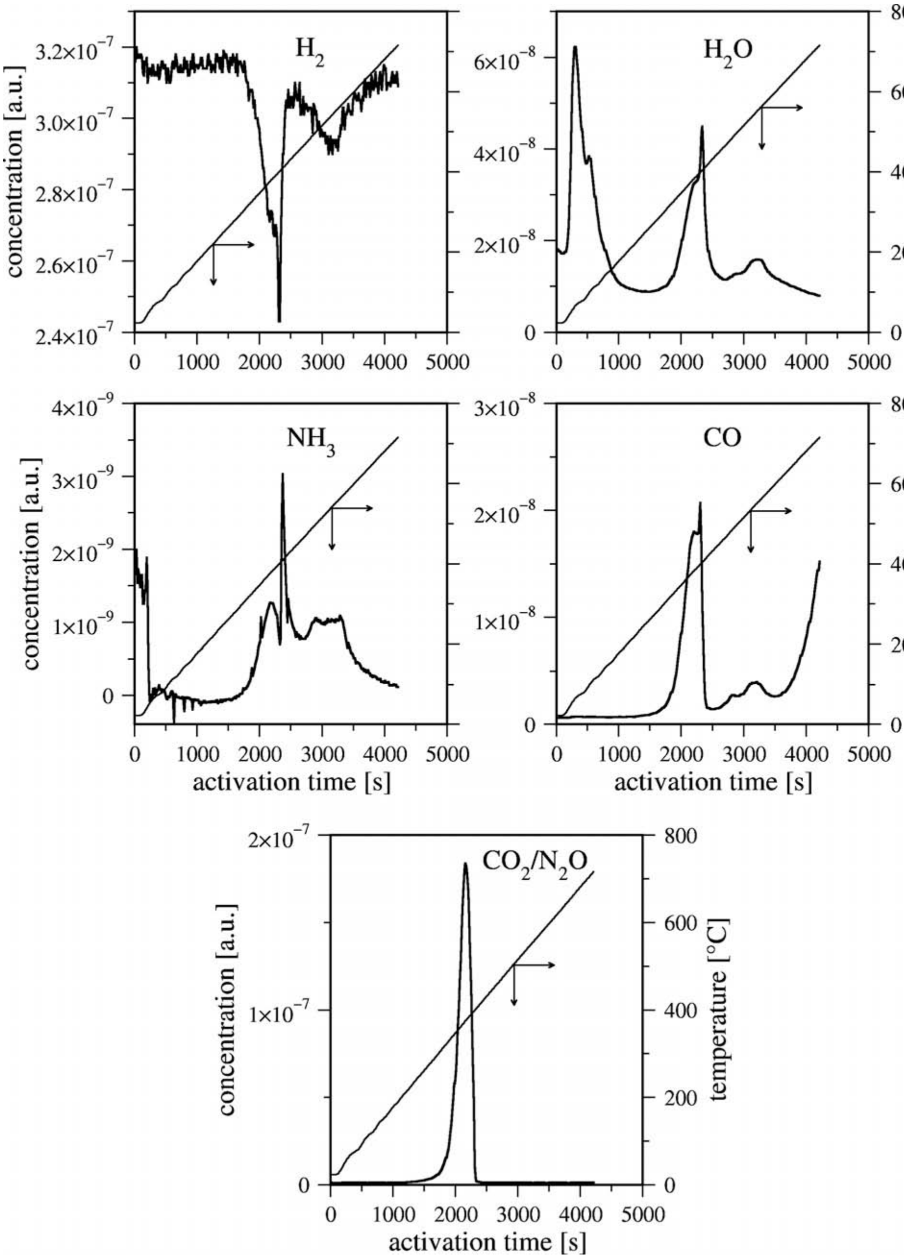

Fig. 5. TPR–MS studies (6% H_2/Ar) of the $Ba(NO_3)_2$/B sample (0.1699 g) that contained 0.0280 g $Ba(NO_3)_2$.

Table 2
Interaction of the Ru/carbon and Ba–Ru/carbon catalysts with oxygen.

Sample	Total O_2 uptake (μmol/g_{C+Ru})	O_2 uptake corresponding to barium (mol O/mol Ba)	FE_{Ru}	d_{Ru} (nm)
Ru9.1/B*	293	–	0.59	1.7
Ba0.36–Ru9.1/B	409	0.64	–	–
Ba0.81–Ru9.1/B	505	0.52	–	–
Ba0.30/B	55.4	0.37	–	–
Ba0.75/B	108	0.29	–	–

* Data taken from [55].

rates "r", corresponding to high NH_3 content, i.e. 8.5 mol%, under the pressure of 63 bar at 400 °C were determined. The influence of the amount of promoter in a system on the catalytic activity of this system in NH_3 synthesis is exhibited in Figs. 6 and 7.

In Fig. 6, it can be observed that the activity of catalysts promoted with barium is significantly higher at 400 °C than at 370 °C. Moreover, the integral reaction rate (r_{int}) strongly depends on the barium content in the Ba–Ru9.1/B system. The shape of the integral reaction rate vs. barium content curve is different than that obtained for caesium-promoted catalysts [55]. The strong influence of barium on the catalyst's activity is clearly visible already when the smallest amount of barium, that is approximately

Table 3
Interaction of the reduced Ba–Ru/carbon catalysts with water vapour.

Sample	H_2 emission (μmol/g_{C+Ru})	Ba reduction degree (Ba^0/Ba_{total}) (mol/mol)
Ru9.1/B*	15	–
Ba0.36–Ru9.1/B	86.5	0.18
Ba0.81–Ru9.1/B	154	0.16
Ba0.30/B	2.5	0.008
Ba0.75/B	7	0.009

* Data taken from [55].

0.15 mmol Ba/g_{C+Ru}, is introduced into the system. The integral reaction rate exhibited by the sample Ba0.16–Ru9.1/B was slightly higher than half of the maximal r_{int} value (obtained for Ba0.81–Ru9.1/B). Above 0.4 mmol Ba/g_{C+Ru}, the changes of the activity are very small, i.e. either a flat maximum or a plateau is reached. The value of the apparent activation energy ($E_{370-400}$ = 92 kJ/mol), calculated from data obtained for barium-doped systems is slightly lower than that corresponding to caesium-promoted catalysts (100 kJ/mol) [55]. Moreover, it does not depend on the barium content.

The results of measurements of the reaction rate conducted in an ammonia-rich stream on Ba–Ru9.1/B catalysts are depicted in Fig. 7. The relation between "*r*" and the barium content of the system is qualitatively the same as that obtained for the integral reaction rate. The minute differences between the curves shown in Figs. 6 and 7 are especially noticeable in the low barium content region. In this region the increase in the reaction rate is slightly slower (Fig. 7) than that in the integral reaction rate (Fig. 6). However, it should be noted that the overall dependence of the activity of the catalyst on the barium content is clear and it does not depend on the method of activity determination. The apparent activation energy obtained on the basis of the reaction rate is 100 kJ/mol.

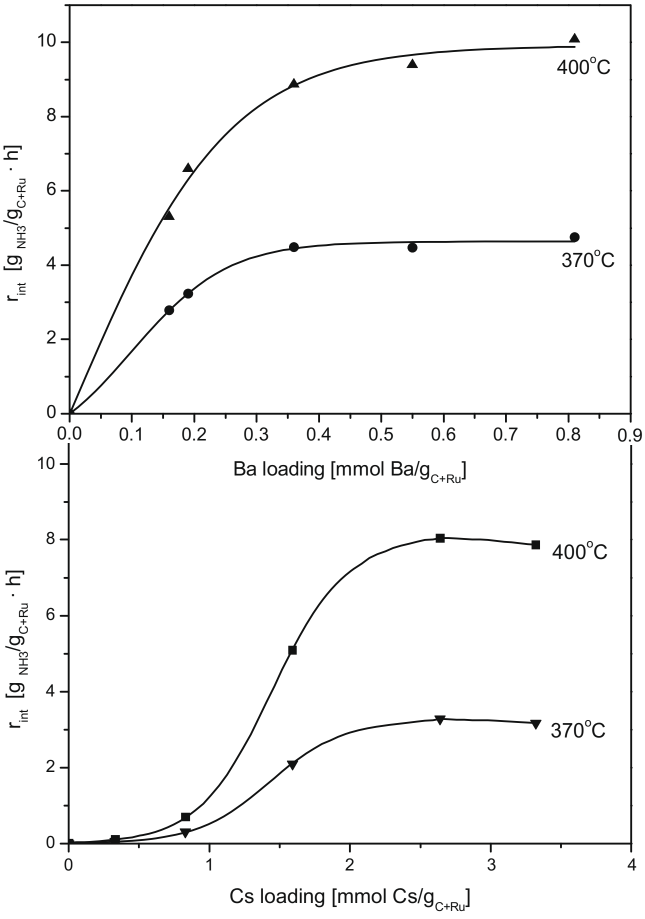

Fig. 6. Ammonia synthesis integral reaction rates (r_{int}) vs. barium content (above) and caesium content (below; data taken from [55]) in the Ru9.1/B catalyst; *p* = 63 bar, H_2:N_2 = 3:1.

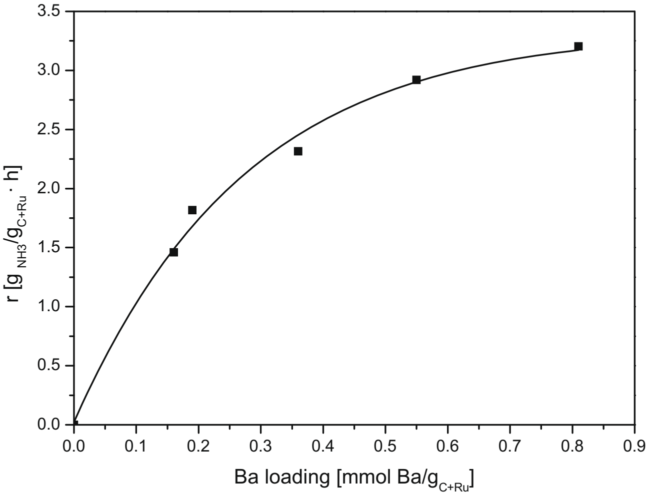

Fig. 7. Rates of ammonia synthesis over barium-promoted Ru9.1/B catalysts vs. the promoter loading; *T* = 400 °C, *p* = 63 bar, H_2:N_2 = 3:1, 8.5% NH_3.

The TOF value corresponding to the Ba0.81–Ru9.1/B sample established based on the average crystallite size of ruthenium and the reaction rate (400 °C, *p* = 63 bar, 8.5% NH_3 gas phase) is 0.098 s^{-1}. It should be emphasized that this value is very high and is similar to the highest activities described in the literature, for example: 0.15 s^{-1} for Ba–Ru/C [33] or 0.145 s^{-1} for Ba–Ru/C [53], compared with 0.019 s^{-1} for Ba–Ru(9.3)/Mg–Al spinel and 0.084 s^{-1} for Ba–Ru(10)/MgO [62].

4. Discussion

Basing on the aforementioned results two issues can be discussed. First of all, the chemical form of the promoter and its location in the working system. Secondly, the promoting mechanism of barium.

The problem of establishing the chemical state of barium in the steady-state conditions of NH_3 synthesis has been investigated by many research groups. Barium hydroxide [52] and barium oxide [1,48,51,52] have been suggested to be the working-state barium-containing species. Signals corresponding to the latter have been found in the diffraction patterns presented in this work (Figs. 1–3). In situ XRD studies have shown that barium nitrate decomposition leads to amorphous barium oxide, which reacts with CO_2 to form $BaCO_3$. Barium carbonate decomposes at temperatures higher than 300 °C. This leads to the formation of BaO. No other barium-containing species are noted in the XRD pattern. However, it is not certain whether crystalline BaO can effectively promote ruthenium. Hansen et al. have suggested that the effect which barium exerts on ruthenium is caused by a thin layer of BaO_x [39,40]. In the diffraction patterns, the signals corresponding to barium oxide indicate a high degree of crystallinity of this compound (Figs. 1–3). It is highly unlikely that these signals correspond to a thin layer. Therefore, on the basis of the results of the in situ XRD studies alone, it is impossible to determine which barium-containing species present in the working state of the catalyst can promote ruthenium. On the contrary to what Hansen et al. [39,40] suggested, it is doubtful whether a nonstoichiometric barium oxide could exist under the ammonia synthesis conditions. This is due to the fact that there are no data in the literature regarding stable barium oxides with a stoichiometry, in which the Ba:O ratio would be different than 1:1 or 1:2. More information regarding the active form of barium can be gained from chemical methods of catalyst characterization.

Studies of the interactions of reduced Ba–Ru/carbon systems with water vapour have shown that after activation, barium is partially reduced. This means that in these samples, a part of the ruthenium surface is covered by metallic barium, which is responsible for the hydrogen evolution. The remaining part of barium is in the form of BaO and does not produce hydrogen upon reaction with $H_2O_{(g)}$. This interpretation is in accordance with the literature data, as Ba^0 and BaO can coexist under highly reductive conditions [52,63], such as those in ammonia synthesis.

The results of the studies concerning the interaction of the catalysts with oxygen seem to support the suggestion that in the working state of the catalyst barium can exist in two forms: Ba^0 and BaO. It can be supposed that, apart from Ru, only Ba^0 can consume oxygen, upon which BaO_2 forms. The literature data suggest that barium oxide does not react with oxygen at 0 °C [58]. However, the values of the O:Ba ratio for Ba0.36–Ru9.1/B and Ba0.81–Ru9.1/B systems (Table 2) are significantly higher than those resulting from the reduction degrees of barium in these systems (Table 3). For example, in the case of Ba0.36–Ru9.1/B, the reduction degree is 0.18, and would therefore require the consumption of 0.36 mol O/mol Ba assuming that all the Ba^0 atoms are transformed to BaO_2. As seen in Table 2, the value of the O:Ba ratio for the Ba0.36–Ru9.1/B sample is 0.64. The magnitude of the difference is too large for the oxygen consumption to be ascribed solely to that transition because the value of oxygen uptake is more than twice higher than 0.36 mol O/mol Ba. In this situation we suppose that only ruthenium can consume the excess amount of oxygen. It is commonly known that barium inhibits the sintering of the active phase crystallites during the reduction of the catalyst [18,23]. Therefore, the amount of oxygen consumed by ruthenium may possibly be higher than that which corresponds to the unpromoted Ru/carbon system. Simple calculations based on the assumption that in the reduced Ba0.36–Ru9.1/B catalyst ruthenium particles are only ~0.2 nm smaller than those reported for the unpromoted sample, i.e. 1.5 nm instead of 1.7 nm in size (Table 2), justify such a speculation. A definite confirmation of this could be gained by performing an in situ TEM study of a sample of the Ba-promoted catalyst in hydrogen, using an instrument with extremely high resolution.

The chemical state of the promoter is not the only important issue which should be considered when discussing the steady state of a catalyst. The location of the promoter in a barium–ruthenium/carbon system is also significant. The shape of the Ba–Ru/carbon catalyst productivity vs. barium content curve (Fig. 6) depends on the location of the promoter in the system. Hence, it is connected with the Ba distribution between the ruthenium surface and that of the carbon support. However, it can be said that the barium-containing species, especially those responsible for the promoting effect of barium, are, even at small concentrations, mainly localized on the surface of ruthenium crystallites. In other words, the heat of Ba adsorption on ruthenium is higher than that on active carbon, and therefore the presence of even small amounts of barium, i.e. even below 0.16 mmol Ba/g_{C+Ru}, introduced into the system gives such marked results. The plateau in the range of 0.4–0.8 mmol Ba/g_{C+Ru} (Fig. 6) indicates that a further increase in the coverage of the ruthenium surface with barium-containing species does not influence the r_{int} value. It is possible that when more than 0.4 mmol Ba/g_{C+Ru} is present in the catalyst, the excess accumulates mainly on the carbon support. This is different than the effect observed in the case of caesium-doped catalysts [55]. The shape of the r_{int} vs. Cs loading curve is of a peculiar S-like shape [55]. Due to very high heat of adsorption at low caesium contents, the Cs_xO_y groups are predominantly located on carbon, whereas the Ru crystallites remain almost uncovered. As a result, a very small promotional effect is observed. As the heat of Cs_xO_y adsorption on carbon falls below a certain value – controlled by the Cs loading, the ruthenium coverage by Cs_xO_y starts to increase dramatically, thus resulting in a dramatic r_{int} increase (the scope of 0.9–2 mmol Cs/g_{C+Ru}). Finally, the Ru coverage by the Cs_xO_y species reaches an optimal value – a full promotional effect [55].

Another issue is the promoting mechanism of barium. As mentioned in Section 1, the opinions regarding this problem differ. An electron promotion has been suggested [3,39,40], as well as a structural one [32,33,53], but also a combination of these effects has been put forward [52]. The results presented in this paper prove that, apart from barium oxide, Ba^0 is also present in the working-state catalyst. Metallic barium can donate electrons to ruthenium and hence, act as an electron promoter. However, the main barium-containing species in the working-state catalyst is barium oxide. Therefore, BaO can cover a significant amount of the surface of ruthenium crystallites [39,40] and thus modify their surface [4,64]. In fact, the geometry of the ruthenium crystallites influences the degree of hydrogen coverage under ammonia synthesis conditions, which determines the amount of free active sites [64–66].

Taking the aforementioned facts into account, one can say that the promoting effect of barium is determined by its chemical state under ammonia synthesis conditions. Distribution of the promoter depends on the competitive interactions between barium and carbon or ruthenium surfaces.

5. Conclusions

Ruthenium promotes the decomposition of barium nitrate deposited onto the surface of Ru/carbon catalysts when heating the samples in a hydrogen-containing stream: in the presence of Ru, the onset of the NO_3^- anion reduction (T_{onset}) is shifted, by about 300 °C, towards lower temperatures. The XRD studies have shown that the only crystalline phase which can be discerned under steady-state conditions is BaO. The results of additional experiments, i.e. interaction with water and oxygen, indicate that in the working state the surface of the catalyst is partly covered with $Ba^0 + BaO$. The promoting effect of barium seems to be of a double nature. The reduced form (Ba^0) influences the electronic properties of the ruthenium surface – electronic promotion, whereas barium oxide affects the structure of the Ru surface – structural promotion. Ba can influence the amount of hydrogen adsorbed on the active phase surface by changing the geometry of ruthenium crystallites. It cannot be excluded that the number and kind of the active sites on the Ru surface can also be changed in the presence of barium.

Acknowledgment

Z. Kowalczyk, W. Raróg-Pilecka and E. Truszkiewicz are grateful to the Foundation for Polish Science for financial support.

References

[1] Z. Kowalczyk, M. Krukowski, W. Raróg-Pilecka, D. Szmigiel, J. Zieliński, Appl. Catal. A-GEN 248 (2003) 67.

[2] X. Zheng, S. Zhang, J. Xu, K. Wei, Carbon 40 (2002) 2597.

[3] I. Rossetti, N. Pernicone, L. Forni, Appl. Catal. A-GEN 208 (2001) 271.

[4] W. Raróg-Pilecka, E. Miśkiewicz, D. Szmigiel, Z. Kowalczyk, J. Catal. 231 (2005) 11.

[5] K. Lubkowski, W. Arabczyk, B. Grzmil, B. Michalkiewicz, A. Pattek-Janczyk, Appl. Catal. A-GEN 329 (2007) 137.

[6] N. Pernicone, E. Ferrero, I. Rossetti, L. Forni, P. Canton, P. Riello, G. Fagherazzi, M. Signoretto, F. Pinna, Appl. Catal. A-GEN 251 (2003) 121.
[7] Hz. Liu, Xn. Li, Ind. Eng. Chem. Res. 36 (1997) 335.
[8] J.R. Jennings (Ed.), Catalytic Ammonia Synthesis: Fundamentals and Practice, Plenum Press, New York, 1991.
[9] S. Hagen, R. Barfod, R. Fehrmann, C.J.H. Jacobsen, H.T. Teunissen, I. Chorkendorff, J. Catal. 214 (2003) 327.
[10] W. Raróg-Pilecka, E. Miśkiewicz, M. Matyszek, Z. Kaszkur, L. Kępiński, Z. Kowalczyk, J. Catal. 237 (2006) 207.
[11] W. Raróg-Pilecka, E. Miśkiewicz, L. Kępiński, Z. Kaszkur, K. Kielar, Z. Kowalczyk, J. Catal. 249 (2007) 24.
[12] W. Raróg-Pilecka, A. Jedynak-Koczuk, J. Petryk, E. Miśkiewicz, S. Jodzis, Z. Kaszkur, Z. Kowalczyk, Appl. Catal. A-GEN 300 (2006) 181.
[13] A. Boisen, S. Dahl, C.J.H. Jacobsen, J. Catal. 208 (2002) 180.
[14] C.J.H. Jacobsen, S. Dahl, B.S. Clausen, S. Bahn, A. Logadottir, J.K. Norskov, J. Am. Chem. Soc. 123 (2001) 8404.
[15] C.J.H. Jacobsen, Chem. Commun. (2000) 1057.
[16] R. Kojima, K. Aika, Chem. Lett. (2000) 514.
[17] I. Rossetti, N. Pernicone, L. Forni, Appl. Catal. A-GEN 248 (2003) 97.
[18] Z. Kowalczyk, S. Jodzis, W. Raróg, J. Zieliński, J. Pielaszek, Appl. Catal. A-GEN 173 (1998) 153.
[19] Z. Kowalczyk, S. Jodzis, W. Raróg, J. Zieliński, J. Pielaszek, A. Presz, Appl. Catal. A-GEN 184 (1999) 95.
[20] C. Liang, Z. Wei, Q. Xin, C. Li, Appl. Catal. A-GEN 208 (2001) 193.
[21] C. Liang, Z. Li, C. Li, J. Catal. 211 (2002) 278.
[22] H.S. Zeng, K. Inazu, K. Aika, Appl. Catal. A-GEN 219 (2001) 235.
[23] Z. Zhong, K. Aika, J. Catal. 173 (1998) 535.
[24] Z. Zhong, K. Aika, Inorg. Chem. Acta 280 (1998) 183.
[25] Z. Li, Ch. Liang, Z. Feng, P. Ying, D. Wang, C. Li, J. Mol. Catal. A 211 (2004) 103.
[26] W. Han, B. Zhao, C. Huo, Hz. Liu, Chin. J. Catal. 25 (2004) 194.
[27] C. Liang, Z. Wei, M. Luo, P. Ying, Q. Xin, C. Li, Stud. Surf. Sci. Catal. 138 (2001) 283.
[28] Z. Kowalczyk, J. Sentek, S. Jodzis, E. Mizera, J. Góralski, T. Paryjczak, R. Diduszko, Catal. Lett. 45 (1997) 65.
[29] K. Aika, T. Takano, S. Murata, J. Catal. 136 (1992) 126.
[30] O. Hinrichsen, F. Rosowski, A. Hornung, M. Muhler, G. Ertl, J. Catal. 165 (1997) 33.
[31] F. Rosowski, A. Hornung, O. Hinrichsen, D. Herein, M. Muhler, G. Ertl, Appl. Catal. A-GEN 151 (1997) 443.
[32] H. Bielawa, O. Hinrichsen, A. Birkner, M. Muhler, Angew. Chem. Int. Ed. 40 (6) (2001) 1061.
[33] D. Szmigiel, H. Bielawa, M. Kurtz, O. Hinrichsen, M. Muhler, W. Raróg, S. Jodzis, Z. Kowalczyk, L. Znak, J. Zieliński, J. Catal. 205 (2002) 205.
[34] S.E. Siporin, R.J. Davis, J. Catal. 222 (2004) 315.
[35] K. Aika, A. Ohya, A. Ozaki, Y. Inoue, I. Yasumori, J. Catal. 92 (1985) 305.
[36] B. Fastrup, Catal. Lett. 48 (1997) 111.
[37] C.J.H. Jacobsen, S. Dahl, P.L. Hansen, E. Törnqvist, L. Jensen, H. Topsøe, D.V. Prip, P.B. Møenshaug, I. Chorkendorff, J. Mol. Catal. A 163 (2000) 19.
[38] S. Dahl, J. Sehested, C.J.H. Jacobsen, E. Törnqvist, I. Chorkendorff, J. Catal. 192 (2000) 391.
[39] T.W. Hansen, P.L. Hansen, S. Dahl, C.J.H. Jacobsen, Catal. Lett. 84 (2002) 7.
[40] T.W. Hansen, J.B. Wagner, P.L. Hansen, S. Dahl, H. Topsøe, C.J.H. Jacobsen, Science 294 (2001) 1508.
[41] C.J.H. Jacobsen, J. Catal. 200 (2001) 1.
[42] D. Szmigiel, W. Raróg-Pilecka, E. Miśkiewicz, E. Maciejewska, Z. Kaszkur, J. Sobczak, Z. Kowalczyk, Catal. Lett. 100 (2005) 79.
[43] R.B. Strait, Nitrogen Methanol 238 (1999) 37.
[44] R.B. Strait, S.A. Knez, in: International Conference Exhibition, Caracas, 28.02–2.03.1999.
[45] G. Ertl, S.B. Lee, M. Weiss, Surf. Sci. 114 (1982) 527.
[46] J.J. Mortensen, B. Hammer, J.K. Norskov, Phys. Rev. Lett. 80 (1998) 4335.
[47] J.K. Norskov, S. Holloway, N.D. Lang, Surf. Sci. 137 (1984) 65.
[48] M. Guraya, S. Sprenger, W. Raróg-Pilecka, D. Szmigiel, Z. Kowalczyk, M. Muhler, Appl. Surf. Sci. 238 (2004) 77.
[49] N.B. Shitova, N.M. Dobrynkin, A.S. Noskov, I.P. Prosvirin, V.I. Bukhtiyarov, D.I. Kochubei, P.G. Tsyrulnikov, D.A. Shlyapin, Kinet. Catal. 45 (2004) 414.
[50] A. Logadottir, T.H. Rod, J.K. Nørskov, B. Hammer, S. Dahl, C.J.H. Jacobsen, J. Catal. 197 (2001) 229.
[51] I. Rossetti, F. Mangiarini, L. Forni, Appl. Catal. A-GEN 323 (2007) 219.
[52] H.S. Zeng, K. Inazu, K. Aika, J. Catal. 211 (2002) 33.
[53] W. Raróg, Z. Kowalczyk, J. Sentek, D. Składanowski, J. Zieliński, Catal. Lett. 68 (2000) 163.
[54] S.R. Tennison, in: J.R. Jennings (Ed.), Catalytic Ammonia Synthesis: Fundamentals and Practice, Plenum Press, New York, 1991, p. 303.
[55] W. Raróg-Pilecka, E. Miśkiewicz, S. Jodzis, J. Petryk, D. Łomot, Z. Kaszkur, Z. Karpiński, Z. Kowalczyk, J. Catal. 239 (2006) 313.
[56] T. Hikita, Y. Kadowaki, K. Aika, J. Phys. Chem. 95 (1991) 9396.
[57] K. Aika, K. Shimazaki, Y. Hattori, A. Ohya, S. Ohshima, K. Shirota, A. Ozaki, J. Catal. 92 (1985) 296.
[58] J.E. Macintyre (Ed.), Dictionary of Inorganic Compounds, Chapman & Hall, London, 1992.
[59] Z. Kaszkur, J. Appl. Cryst. 33 (2000) 1262.
[60] Z. Kowalczyk, Catal. Lett. 37 (1996) 173.
[61] Z. Kowalczyk, W. Raróg-Pilecka, Przem. Chem. 85/2 (2006) 124.
[62] D. Szmigiel, W. Raróg-Pilecka, E. Miśkiewicz, M. Gliński, M. Kielak, Z. Kaszkur, Z. Kowalczyk, Appl. Catal. A-GEN 273 (2004) 105.
[63] P. Pascal (Ed.), Nouveau traité de chimie minérale, tom 4, Masson et C^{ie}, Paris, 1958, p. 749.
[64] S.E. Siporin, R.J. Davies, J. Catal. 225 (2004) 359.
[65] C.Y. Fan, K. Jacobi, Surf. Sci. 482–485 (2001) 21.
[66] K. Christmann, U. Muschiol, Z. Phys. Chem. 197 (1996) 155.